

DOI: 10.17148/IJIREEICE.2025.131023

OFF-BOARD ELECTRIC VEHICLE BATTERY CHARGER USING PV ARRAY

RAVADA. GOPAL¹, U. LAKSHMI²

PG Student, Department of Electrical Engineering, Sankethika Vidya Parishad Engineering College, Andhra Pradesh,
India¹

Assistant Professor, Department of Electrical Engineering, Sankethika Vidya Parishad Engineering College,

Andhra Pradesh, India²

Abstract: In the past decade, the automobile sector has experienced significant growth due to the advancement of electric vehicles (EVs). The battery charging system is crucial for the progress of EVs. Charging EV batteries from the grid increases the demand on the load. Consequently, this study proposes a photovoltaic (PV) array-based off-board EV battery charging system. Regardless of solar irradiance levels, the EV battery must be charged consistently, which is accomplished by incorporating a backup battery bank alongside the PV array. By utilizing a sepic converter and a three-phase bidirectional DC–DC converter, the proposed system can charge the EV battery during both sunny and non-sunny periods. During peak sunlight hours, the backup battery charges in conjunction with the EV battery, while during non-sunny hours, the backup battery facilitates the charging of the EV battery. The proposed charging system has been simulated using Simulink within the MATLAB software, and an experimental prototype has been constructed and tested in the laboratory, with the results presented in this study.

I. INTRODUCTION

The escalating impact of greenhouse gases emitted by conventional IC engines has raised significant environmental concerns. This situation has contributed to the rapid growth of pollution-free electric vehicles (EVs) within the automotive sector [1–3]. Nevertheless, charging EV batteries from the utility grid increases the demand on the grid, ultimately leading to higher electricity costs for EV owners, which necessitates the exploration of alternative energy sources [4, 5]. Given the inexhaustible and environmentally friendly characteristics of renewable energy sources (RESs), they can be utilized to charge EV batteries. Consequently, EVs powered by RESs can be classified as 'green transportation' [6]. Solar energy is one of the most promising RESs, easily harnessed to charge EV batteries [7, 8]. Therefore, in the proposed system, photovoltaic (PV) array power is employed to charge the EV battery using various power converter topologies.

Lithium-ion batteries are commonly utilized in EVs due to their high power density, efficiency, lightweight design, and compact size [9, 10]. Additionally, these batteries support fast charging and possess a long lifecycle with a low selfdischarge rate. They also present a minimal risk of explosion in cases of overcharging or short-circuiting. During the charging process, these batteries necessitate precise voltage control. As a result, various power electronic converters equipped with voltage controllers are implemented for the charging of EV batteries. Due to the intermittent characteristics of the photovoltaic (PV) array, it is necessary to utilize power converters for charging the electric vehicle (EV) battery. Among the various types of converters, multiport converters (MPCs) are favored in the onboard chargers of hybrid EVs because of their ability to connect power sources and energy storage components such as PV arrays, ultracapacitors, supercapacitors, fuel cells, and batteries to the loads in the EV, which include the motor, lights, power windows and doors, radios, amplifiers, and mobile phone chargers. However, MPCs have the disadvantage of increasing the weight, cost, and maintenance requirements of the EV, as all sources are integrated within the vehicle itself. Additionally, the complexity of implementing controllers rises in these converter-based EV battery charging systems [11-13]. Therefore, this paper proposes an off-board charger where the EV battery is housed within the vehicle unit, while the PV array and backup battery bank are situated at the charging or parking station. Various converter topologies for off-board charging systems have been discussed in the literature [14–16]. Among the different converter topologies, the sepic converter is preferred due to its ability to operate in both boost and buck modes. It also offers the benefits of having the same input and output voltage polarity, low input current ripple, and reduced electromagnetic interference (EMI) [17, 18]. Nevertheless, during periods of low solar irradiation and at night, an additional storage battery bank is necessary to charge the EV battery. This backup battery bank must be charged in the forward direction and discharged in the reverse direction, depending on the solar irradiation levels. Consequently, a bidirectional converter that allows power flow in both directions is essential [19]. Bidirectional converters are categorized into non-isolated and isolated types. In isolated converters, the transformer provides isolation, which consequently increases the converter's price, weight, and size. Given that weight and size are critical concerns for electric vehicles (EVs), non-isolated bidirectional converters are more suitable for this



DOI: 10.17148/IJIREEICE.2025.131023

application [20–22]. Among the various topologies of non-isolated bidirectional converters, the bidirectional interleaved DC–DC converter (BIDC) is favored due to its benefits, such as enhanced efficiency in discontinuous conduction mode, minimal inductance values, and reduced ripple current achieved through the multiphase interleaving technique. The inclusion of a snubber capacitor across the switches mitigates turnoff losses, while the zero voltage resonant soft switching technique diminishes the parasitic ringing effect of the inductor current. These features represent additional advantages of this bidirectional converter [23–25]. The system described in [25] is an off-board EV battery charging solution that utilizes power from a photovoltaic (PV) array to charge the EV battery via a bidirectional DC–DC converter while in a stationary state. During operation, the EV battery discharges to supply power to the DC load. However, this system is limited to charging the EV battery only during daylight hours. To address this limitation and enable uninterrupted charging of the EV battery, a proposed charger has been developed, integrating a PV array with a sepic converter, a bidirectional DC–DC converter, and a backup battery bank for the purpose of charging the EV battery.

II. OPERATION OF THE PROPOSED SYSTEM

The proposed photovoltaic-electric vehicle (PV-EV) battery charger comprises a photovoltaic (PV) array, a sepic converter, a half-bridge bidirectional DC-DC converter (BIDC), an electric vehicle (EV) battery, a backup battery bank, and a controller, as illustrated in Fig. 1. The controller is responsible for generating gate pulses for the sepic converter to achieve a constant output voltage at the DC link. Additionally, it generates gate pulses for the BIDC switches to operate in boost mode for charging the backup battery from the PV array and in buck mode for charging the EV battery from the backup battery. Furthermore, the controller produces gate pulses for the auxiliary switches Sa, Sb, and Sc. Under conditions of high solar irradiation, all auxiliary switches are activated to connect the DC link with the PV array via the sepic converter, the DC link with the backup battery through the BIDC, and the DC link with the EV battery. Conversely, when solar irradiation is low, switch Sa is deactivated, thereby isolating the PV array and sepic converter from the DC link. Similarly, switch Sc is turned off to disconnect the BIDC and backup battery from the DC link when solar power is inadequate to charge the backup battery. The proposed system functions in three distinct modes, namely mode 1, mode 2, and mode 3, as detailed in this section.

III. DESIGN OF THE CONVERTERS USED IN THE PROPOSED CHARGER

In the proposed charging system, the sepic converter delivers a constant output voltage regardless of the PV array voltage by modifying its duty ratio through the PI controller. The sepic converter is composed of one IGBT switch, one diode, two inductors, and two capacitors, as illustrated in Fig. 2. The primary benefits of the sepic converter include: (i) its ability to function in both boost and buck modes based on the duty ratio; (ii) it supplies the output voltage with the same polarity as the input voltage, in contrast to buck—boost and cuk converters [16]. The voltage gain of the sepic converter is expressed by the following equation:

$$\frac{V_{dc}}{V_{pp}} = \frac{D}{1-D} \tag{1}$$

where Vdc represents the direct current link voltage, VPV denotes the voltage of the photovoltaic array, and D signifies the duty ratio of the SEPIC converter. The inductor and capacitor values for the SEPIC converter are selected according to equations (2)–(4) [17]:

$$L_a = L_b = \frac{v_{PVmin} D_{max}}{2\Delta i_{PV} f_{sw}} \tag{2}$$

$$C_1 = \frac{I_{dc}D_{max}}{\Delta V_{C1}f_{sw}} \tag{3}$$

$$C_2 = \frac{I_{dc}D_{max}}{\Delta V_{dc}f_{sw}} \tag{4}$$



DOI: 10.17148/IJIREEICE.2025.131023

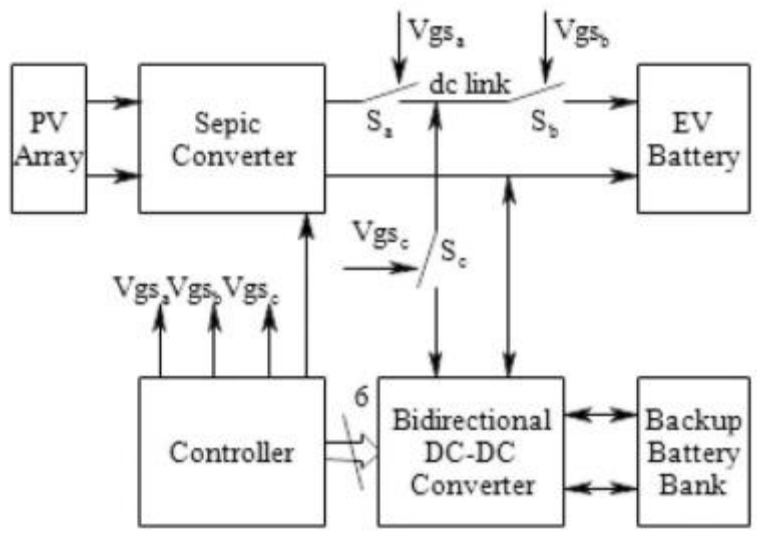


Fig.1 Block diagram of the EV battery charger

Currently, $\Delta VC1$ represents the voltage ripple across capacitor C1, ΔVdc denotes the output voltage ripple, and Dmax signifies the maximum duty ratio, which is calculated as follows:

$$D_{max} = \frac{V_{dc} + V_D}{V_{PVmin} + V_{dc} + V_D}$$
 (5)

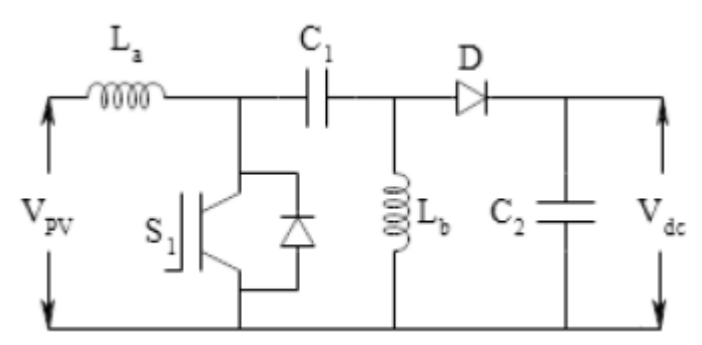


Fig.2 Schematic diagram of sepic converter

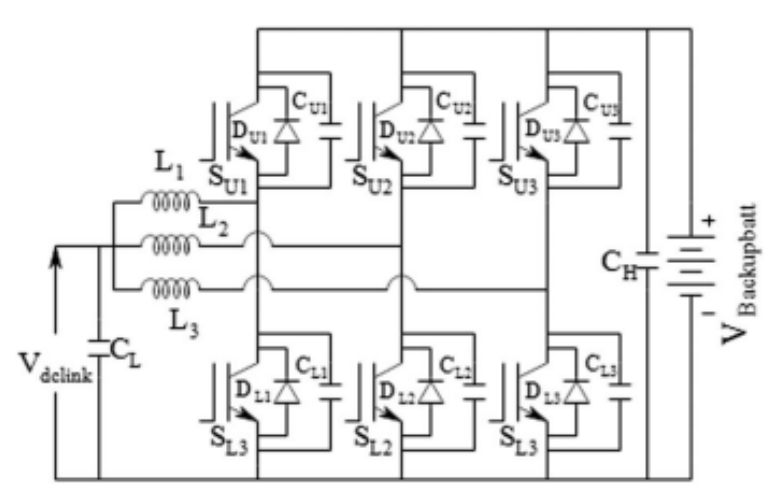


Fig.3 Schematic diagram of half-bridge BIDC

Figure 3 illustrates the schematic representation of the BIDC utilized in the proposed charging system. The backup battery bank is situated on the high voltage side, while the dc link is positioned on the low voltage side of the converter. This



DOI: 10.17148/IJIREEICE.2025.131023

converter functions in boost mode when operating in the forward direction and in buck mode when functioning in the reverse direction. In boost mode, the active switches are SL1, SL2, and SL3, whereas in buck mode, the active switches are SU1, SU2, and SU3. Each switch in this converter is accompanied by an antiparallel diode and a parallel snubber capacitor. During boost mode, the inductors L1, L2, and L3 serve as boost inductors, while they function as a low-pass filter in buck mode. The capacitors, CL and CH, act as the smoothing energy buffer components of this converter. The interleaved inductor currents help to reduce the ripples in the current. The operational modes of the converter are examined by analyzing the performance of a single leg converter as referenced in [20]. The voltage conversion ratios for the BIDC in both boost and buck modes are provided in equations (6) and (7), respectively.

$$\frac{V_{BackBatt}}{V_{dc}} = \frac{1}{1 - D_{Boost}} \tag{6}$$

$$\frac{V_{dc}}{V_{BackBatt}} = D_{Buck} \tag{7}$$

where VBackupBatt represents the voltage of the backup battery and DBoost denotes the duty ratio of BIDC in boost mode, while DBuck refers to the duty ratio in buck mode. The inductor values are assumed to be lower than the critical inductance values in both boost and buck modes to enable the converter to function in discontinuous conduction mode, thereby enhancing efficiency [20]. The critical inductance values for both boost and buck modes are determined using equations (8) and (9), respectively.

$$L_{cric} = \frac{3V^2_{BackupBatt}D_{Boost}(1 - D_{Boost})^2}{2Pf_S}$$
 (8)

$$L_{cric} = \frac{3V_{dc}^2(1 - D_{Buck})}{2Pf_S} \tag{9}$$

$$C_H = \frac{D_{Boost}P}{2f_S^{V^2}BackupBatt} \tag{10}$$

$$C_L = \frac{V_{BackupBatt}D_{Buck}(1 - D_{Buck})}{8f^2_{s}L\Delta V_{dc}}$$
 (11)

IV. DESIGN OF CONTROLLERS

The controller of the proposed charger produces gate pulses for the switches located in the sepic converter, BIDC, and the three auxiliary switches. The algorithm for activating and deactivating the auxiliary switches is illustrated in Fig. 4. The controller monitors the voltage and current of the PV array and calculates the power generated by it. If the power from the PV array exceeds the rated power of the EV battery, PR, the controller issues gate pulses to activate all auxiliary switches, allowing both the EV battery and the backup battery bank to be charged simultaneously from the PV array. In cases where the power from the PV array is less than the rated power of the EV battery but greater than the minimum required power, PM, the switch Sc is deactivated, disconnecting the backup battery from the charging system, while switches Sa and Sb are activated to charge only the EV battery from the PV array. If the power from the PV array falls below the minimum required power, PM, switch Sa is turned off to isolate the PV array and the sepic converter from the charging system. Meanwhile, switches Sb and Sc are activated to enable the backup battery to charge the EV battery. The proposed charging system employs a PI voltage controller to generate gate pulses for the MOSFET in the sepic converter, ensuring a constant voltage at the DC link, regardless of fluctuations in the PV array voltage. BIDC consists of three legs, each containing two switches. Gate pulses must be supplied to the two switches within the same leg, with a phase difference of 180° between them.



DOI: 10.17148/IJIREEICE.2025.131023

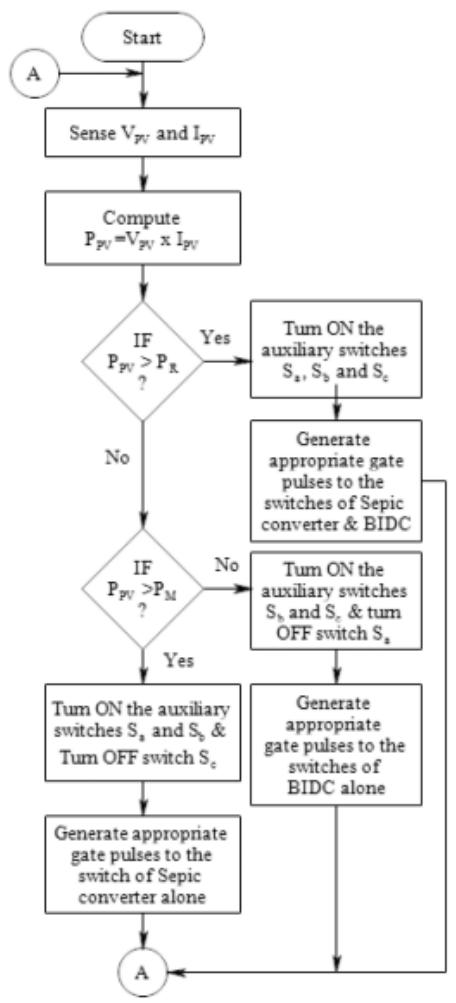


Fig. 4 Flowchart of gate pilses generation for the auxiliary switches

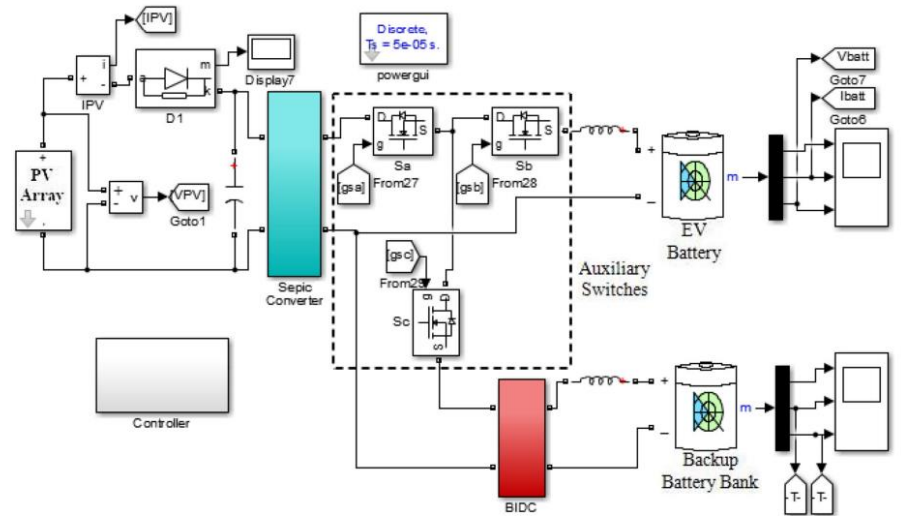


Fig.5 Simulation model of the proposed charger.

The controller in the proposed system produces six gate pulses for the BIDC based on the power generated by the PV array. When the power from the PV array exceeds PR, gate pulses are issued to the BIDC switches to enable operation in boost mode, thereby increasing the dc link voltage to charge the backup battery bank. In this mode, gate pulses are sent to the switches of leg 1 with a 0° phase, while the switches of leg 2 receive pulses with a 120° phase shift relative to those



DOI: 10.17148/IJIREEICE.2025.131023

of leg 1, and the switches of leg 3 are provided with pulses that have a 240° phase shift from those of leg 1. Conversely, if the power from the PV array falls below PM, the gate pulses are generated to operate the BIDC in buck mode, resulting in a step-down voltage at the dc link that is adequate to charge the EV battery using the backup battery. In this configuration, the gate pulses are directed to the switches of leg 3 with a 0° phase, while the gate pulses for the switches of leg 2 and leg 1 are phase shifted by 120° and 240°, respectively, in relation to the pulses of leg 3.

V. MATHEMATICAL MODELLING OF PROPOSED SYSTEM

The mathematical model of the proposed system is developed by integrating the state-space average model of the Sepic converter with that of the Bidirectional DC–DC converter. This model is derived by taking into account the ON and OFF switching periods of the converters [26, 27]. The state-space matrices for the Sepic converter, including the state matrix 'A', input matrix 'B', output matrix 'C', and feed forward matrix 'D', are determined where Req represents the equivalent impedance at the DC link and Ds denotes the duty ratio of the Sepic converter.

$$A = \begin{bmatrix} 0 & 0 & \frac{-(1-D_S)}{L_B} & \frac{-(1-D_S)}{L_B} \\ 0 & 0 & L_B & \frac{-(1-D_S)}{L_B} & \frac{-(1-D_S)}{L_B} \\ \frac{(1-D_S)}{c_1} & \frac{CD_S}{c_1} & \frac{D_S}{L_B} & \frac{L_B}{c_1} \\ \frac{(1-D_S)(1-D_S)}{c_2} & 0 & 0 & \frac{-1}{c_2 R_{eq}} \end{bmatrix}$$
(12)

$$B = \begin{bmatrix} \frac{1}{L_a} \\ 0 \\ 0 \\ 0 \end{bmatrix} \tag{13}$$

$$c = [0001] \tag{14}$$

$$D = [0] \tag{15}$$

where L = (L1/3), Rlp = (RL1/3), and Req1 represents the equivalent impedance across capacitor CH. Rdson denotes the MOSFET turn-on resistance, while RL1 signifies the parasitic resistance of inductor L1. Additionally, DBIDC refers to the duty ratio of BIDC.

$$A_{1} = \begin{bmatrix} \frac{-(R_{lp} + R_{dson})}{L} & 0 & \frac{-(1 - D_{BIDC})}{L} \\ \frac{-1 + 2D_{BIDC}}{C_{L}} & 0 & 0 \\ \frac{(1 - D_{BIDC})}{C_{H}} & 0 & \frac{-1}{C_{H}R_{eq1}} \end{bmatrix}$$
(16)

$$B_1 = \begin{bmatrix} \frac{1}{L} \\ 0 \\ 0 \end{bmatrix} \tag{17}$$

$$C_1 = [001] \tag{18}$$

$$D_1 = [0] \tag{19}$$

The transfer functions of the converters are derived from the aforementioned state-space models, which are then integrated to yield the overall transfer function of the proposed system. The frequency response of this system demonstrates a positive gain margin and phase margin, indicating the stability of the proposed system. Simulation studies for the proposed charger have been conducted, and the results are presented in the subsequent section.



DOI: 10.17148/IJIREEICE.2025.131023

VI. SIMULATION STUDIES AND RESULTS

Simulink, a component of the MATLAB software, is utilized for conducting simulation studies of the proposed system. The PV array is modeled using its classical equation [28, 29]. The Sepic and BIDC converters are constructed using power MOSFETs, inductors, and capacitors that are accessible in the SimPowerSystems Blockset within the Simulink library. The controller is designed using a PWM generator, pulse generator, logic gates, comparator, multiplier, and PI controller, all of which are available in the Simulink library. The PV array model is integrated with the developed Sepic converter and BIDC, along with the battery models found in the Simulink library, to create the proposed charging system, as illustrated in Fig. 5.

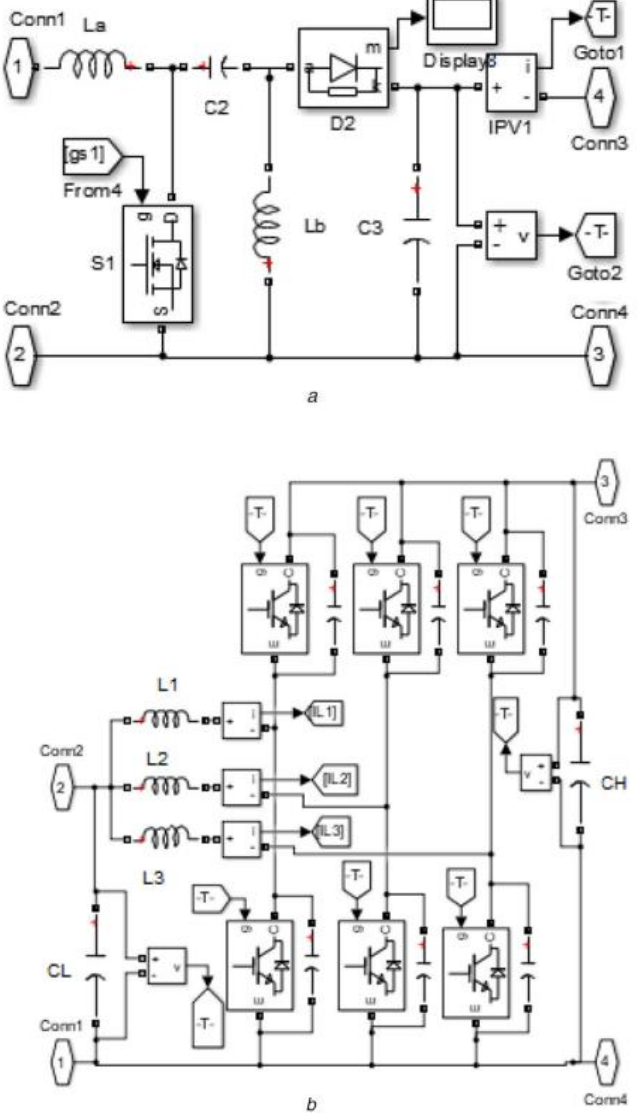


Fig. 6 Simulation model of (a) Sepic conveter, (b) BIDC

The simulation model developed for the sepic converter and BIDC, illustrated as subsystems in Fig. 5, is represented in Figs. 6a and b, respectively. The dynamic response of the system was analyzed using the developed simulation model under PV array irradiation levels of 850, 100, and 500 W/m2 in modes 1, 2, and 3, respectively. The simulation results, which display the voltage and current waveforms of the PV array along with the gate pulses for the auxiliary switches, are shown in Fig. 7. The irradiation waveforms are presented on a scale of 1 for 1000 W/m2 in Fig. 7. Consequently, both the EV battery and the backup battery are charged simultaneously in this mode. In contrast, at a low irradiation level of 100 W/m2, the gate pulses for the auxiliary switches, Vgsb and Vgsc, are high, while the gate pulse Vgsa is low due to the insufficient power from the PV array for charging the EV battery. Therefore, the backup battery bank discharges through the BIDC to charge the EV battery in this mode. During the irradiation of 500 W/m2, the auxiliary switches Sa



IJIREEICE

DOI: 10.17148/IJIREEICE.2025.131023

and Sb are activated, while switch Sc is deactivated, disconnecting the backup battery from the system. Since the power from the PV array is adequate only for charging the EV battery, the backup battery remains isolated and is not charged in this mode. Fig. 7 indicates that the gate pulses to switch Sb remain consistently high as the EV battery is continuously charged across all three modes. If the EV battery reaches full charge, it is isolated from the charging system by turning off switch Sb to prevent trickle charging of the EV battery.

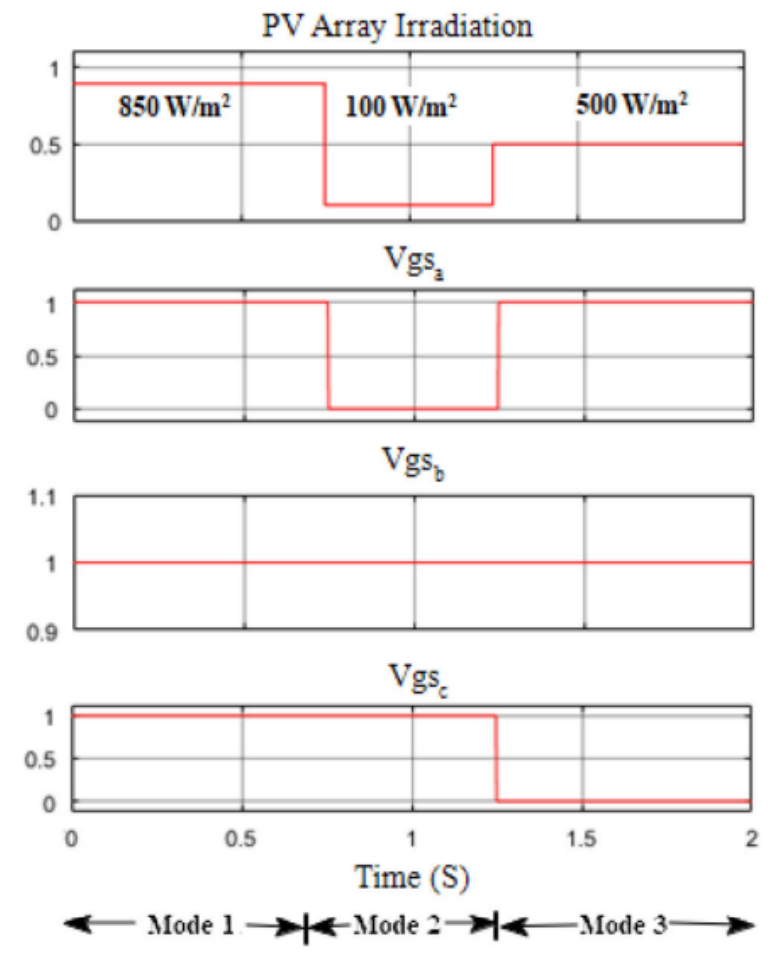


Fig. 7 Waveforms of PV array irradiation and gate pulse to the auxiliary switchs

Figure 8 illustrates the simulated dynamic waveforms of the photovoltaic (PV) array, the direct current (dc) link, the electric vehicle (EV) battery, and the backup battery corresponding to the various irradiation values. In mode 1, the voltage of the PV array, VPV, which is 33.3 V, is reduced to the dc link voltage, Vdc, of 28 V through a sepic converter, as demonstrated in Figures 8a and 8b. The increase in the state of charge (SOC) of the EV battery, along with its negative current depicted in Figure 8c, signifies that the EV battery is undergoing charging in this mode. The Bidirectional DC-DC Converter (BIDC) functions as a boost converter in the forward direction during this mode, elevating the dc link voltage, Vdc, from 28 V to 60.6 V to facilitate the charging of the backup battery, as illustrated in Figure 8d. In mode 2. which occurs during non-sunshine hours and under low irradiation conditions, the PV array becomes isolated, causing the PV array voltage, VPV, to rise to its open circuit voltage of 37.25 V, while the PV array current, IPV, drops to 0 A, as represented by the waveforms of the PV array voltage and current in Figure 8a. During this phase, the BIDC operates in buck mode in the reverse direction, reducing the voltage of the backup battery to 27.32 V to charge the EV battery, as shown in Figure 8c. The positive current and the decrease in the SOC of the backup battery, illustrated in Figure 8d, indicate that the backup battery is being discharged in this mode. By the conclusion of this mode, the voltage of the backup battery decreases from 60.6 V to 55.2 V, as depicted in Figure 8d.



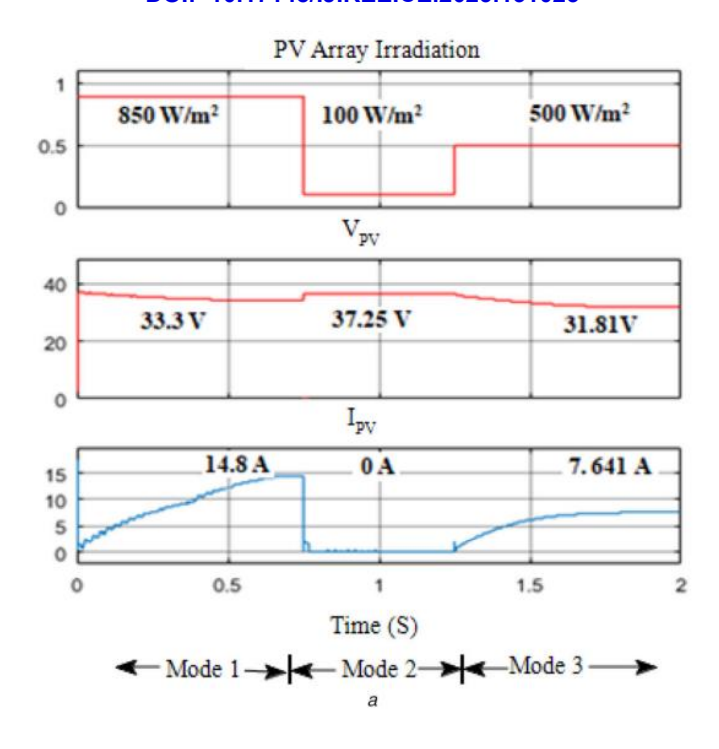
IJIREEICE

International Journal of Innovative Research in Electrical, Electronics, Instrumentation and Control Engineering
Impact Factor 8.414

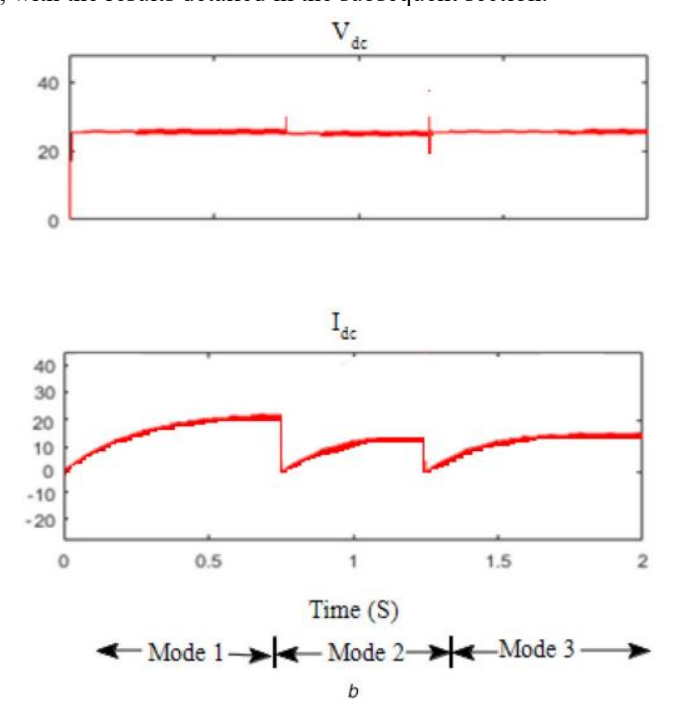
Refereed journal

Vol. 13, Issue 10, October 2025

DOI: 10.17148/IJIREEICE.2025.131023



In mode 3, the voltage of the PV array, VPV, which is 31.81 V, is reduced to a dc link voltage, Vdc, of 27.6 V to facilitate the charging of the EV battery, as illustrated in Figs. 8a and b. During this mode, the state of charge (SOC) of the EV battery is on the rise, and the current is negative, signifying that the EV battery is being charged. Furthermore, in mode 3, since the backup battery is disconnected from the charging system, its voltage remains at the previous level of 55.2 V, and the current drops to zero, as depicted in Fig. 8d. Fig. 8c demonstrates that the SOC of the EV battery is increasing, with negative current observed across all three modes, indicating that the EV battery is continuously charged either by the PV array or the backup battery. The interleaved inductor current waveforms of the Bidirectional DC-DC Converter (BIDC) across all operational modes are presented in Fig. 9. The reversal of inductor current flow in mode 2 clearly signifies that the backup battery is discharging in this mode, while the absence of inductor current in mode 3 indicates that the BIDC is no longer connected to the charger. To corroborate the simulation findings, a hardware prototype has been developed and tested, with the results detailed in the subsequent section.



IJIREEICE

International Journal of Innovative Research in Electrical, Electronics, Instrumentation and Control Engineering
Impact Factor 8.414

Refereed journal

Vol. 13, Issue 10, October 2025

DOI: 10.17148/IJIREEICE.2025.131023

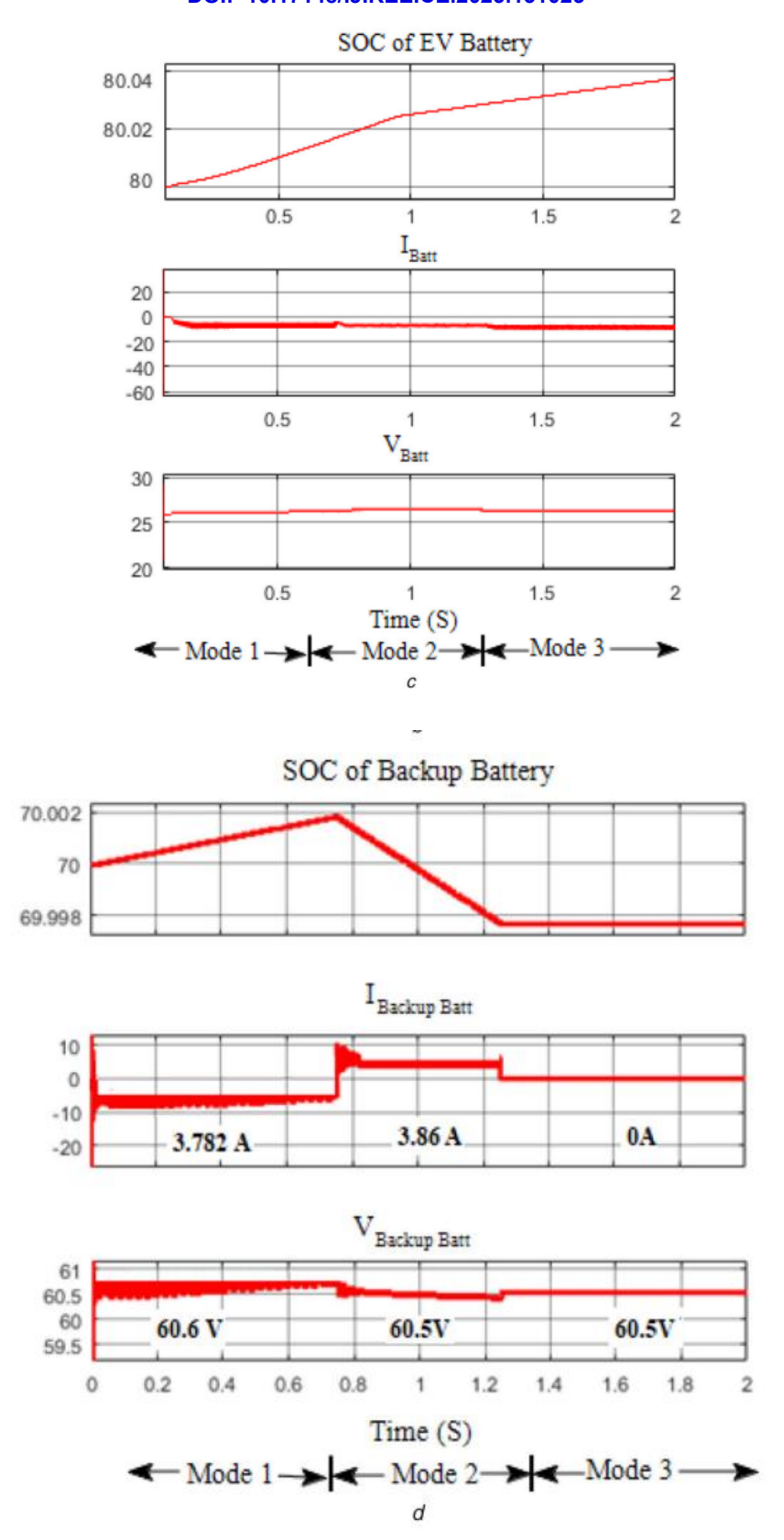


Fig. 8 Waveforms of (a) PV array voltage, VPV & PV array current, IPV, (b) DC link voltage, Vdc, & current, Idc, (c) EV battery SOC, EV battery current, IBatt & EV battery voltage, VBatt, (d) Backup battery SOC, backup battery current, IBackup Batt & backup battery voltage, VBackup Batt



DOI: 10.17148/IJIREEICE.2025.131023

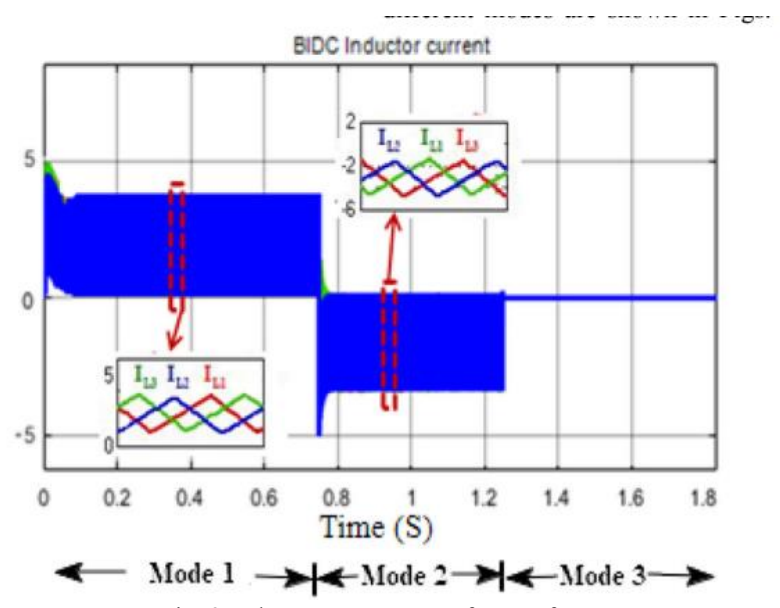


Fig. 9 Inductor current waveforms of BIDC

VII. CONCLUSION

This paper presents a proposed off-board electric vehicle (EV) battery charging system powered by a photovoltaic (PV) array. It examines the system's capability to continuously charge the EV battery regardless of varying irradiation conditions. The design and simulation of the system are conducted within the Simulink environment of MATLAB software. A hardware prototype has been constructed and tested in a laboratory setting for the three distinct operational modes of the proposed charging system, with the results documented. Additionally, experimental investigations are performed using the OPAL-RT Real-Time Simulator OP4500, employing the Real-Time Control Protocol (RCP) methodology, and the dynamic response of the system is provided for both simulation and experimental studies. The correlation between the simulation and experimental findings highlights the effectiveness of the proposed charger.

REFERENCES

- [1]. Santhosh, T.K., Govindaraju, C.: 'Dual input dual output power converter with one-step-ahead control for hybrid electric vehicle applications', IET Electr. Syst. Transp., 2017, 7, (3), pp. 190–200
- [2]. Shukla, A., Verma, K., Kumar, R.: 'Voltage-dependent modelling of fast charging electric vehicle load considering battery characteristics', IET Electr. Syst. Transp., 2018, 8, (4), pp. 221–230
- [3]. Wirasingha, S.G., Emadi, A.: 'Pihef: plug-in hybrid electric factor', IEEE Trans. Veh. Technol., 2011, 60, pp. 1279–1284
- [4]. Kirthiga, S., Jothi Swaroopan, N.M.: 'Highly reliable inverter topology with a novel soft computing technique to eliminate leakage current in grid-connected transformerless photovoltaic systems', Comput. Electr. Eng., 2018, 68, pp. 192–203
- [5]. Badawy, M.O., Sozer, Y.: 'Power flow management of a grid tied PV-battery system for electric vehicles charging', IEEE Trans. Ind. Appl., 2017, 53, pp. 1347–1357
- [6]. Van Der Meer, D., Chandra Mouli, G.R., Morales-Espana Mouli, G., et al.: 'Energy management system with PV power forecast to optimally charge EVs at the workplace', IEEE Trans. Ind. Inf., 2018, 14, pp. 311–320
- [7]. Xavier, L.S., Cupertino, A.F., Pereira, H.A.: 'Ancillary services provided by photovoltaic inverters: single and three phase control strategies', Comput. Electr. Eng., 2018, 70, pp. 102–121
- [8]. Krithiga, S., Ammasai Gounden, N.: 'Investigations of an improved PV system topology using multilevel boost converter and line commutated inverter with solutions to grid issues', Simul. Model. Pract. Theory, 2014, 42, pp. 147–159
- [9]. Sujitha, N., Krithiga, S.: 'RES based EV battery charging system: a review', Renew. Sustain. Energy Rev., 2017, 75, pp. 978–988
- [10]. Farzin, H., Fotuhi-Firuzabad, M., Moeini-Aghtaie, M.: 'A practical scheme to involve degradation cost of lithium-ion batteries in vehicle-to-grid applications', IEEE Trans. Sustain. Energy, 2016, 7, pp. 1730–1738
- [11]. Zubair, R., Ibrahim, A., Subhas, M.: 'Multiinput DC–DC converters in renewable energy applications an overview', Renew. Sustain. Energy Rev., 2015, 41, pp. 521–539



IJIREEICE

International Journal of Innovative Research in Electrical, Electronics, Instrumentation and Control Engineering Impact Factor 8.414 Refereed journal Vol. 13, Issue 10, October 2025

DOI: 10.17148/IJIREEICE.2025.131023

- [12]. Duong, T., Sajib, C., Yuanfeng, L., et al.: 'Optimized multiport dc/dc converter for vehicle drive trains: topology and design optimization', Appl. Sci., 2018, 1351, pp. 1–17
- [13]. Santhosh, T.K., Natarajan, K., Govindaraju, C.: 'Synthesis and implementation of a multi-port dc/dc converter for hybrid electric vehicles', J. Power Electron., 2015, 15, (5), pp. 1178–1189
- [14]. Hongfei, W., Peng, X., Haibing, H., et al.: 'Multiport converters based on integration of full-bridge and bidirectional dc-dc topologies for renewable generation systems', IEEE Trans. Ind. Electron., 2014, 61, pp. 856– 869
- [15]. Shi, C., Khaligh, A.: 'A two-stage three-phase integrated charger for electric vehicles with dual cascaded control strategy', IEEE J. Emerging Sel. Topics Power Electron., 2018, 6, (2), pp. 898–909
- [16]. Chiang, S.J., Shieh, H., Chen, M.: 'Modeling and control of PV charger system with SEPIC converter', IEEE Trans. Ind. Electron., 2009, 56, (11), pp. 4344–4353
- [17]. Falin, J.: 'Designing DC/DC converters based on SEPIC topology', Analog Appl. J., 2008, 4Q, pp. 18–23. Available at https://e2echina.ti.com/cfs-file/ __key/telligent-evolution-components-attachments/ 13-112-00-00-00-00-58-20/Designing-DC-DC-converters-based-on-SEPICtopology.pdf
- [18]. Banaei, M.R., Sani, S.G.: 'Analysis and implementation of a new SEPICbased single-switch buck-boost DC-DC converter with continuous input current', IEEE Trans. Power Electron., 2018, 33, (12), pp. 10317–10325
- [19]. Singh, A.K., Pathak, M.K.: 'Single-stage ZETA-SEPIC-based multifunctional integrated converter for plug-in electric vehicles', IET Electr. Syste. Transp., 2018, 8, (2), pp. 101–111
- [20]. Du, Y., Zhou, X., Bai, S., et al.: 'Review of non-isolated bi-directional DCDC converters for plug-in hybrid electric vehicle charge station application at municipal parking decks'. 2010 Twenty-Fifth Annual IEEE Applied Power Electronics Conf. Exposition, Palm Springs, CA, USA., 2010, pp. 1145–1151
- [21]. Kwon, M., Oh, S., Choi, S.: 'High gain soft-switching bidirectional DC–DC converter for eco-friendly vehicles', IEEE Trans. Power Electron., 2014, 29, pp. 1659–1666
- [22]. Mirzaei, A., Jusoh, A., Salam, Z., et al.: 'Analysis and design of a high efficiency bidirectional DC–DC converter for battery and ultracapacitor applications', Simul. Model. Pract. Theory, 2011, 19, pp. 1651–1667
- [23]. Han, J.T., Lim, C.-S., Cho, J.-H., et al.: 'A high efficiency non-isolated bidirectional DC-DC converter with zero-voltage-transition'. 2013 39th Annual Conf. IEEE Industrial Electronics Society, 2013, pp. 198–203
- [24]. Zhang, J., Lai, J.-S., Kim, R.-Y., et al.: 'High-power density design of a softswitching high-power bidirectional DC–DC converter', IEEE Trans. Power Electron., 2007, 22, pp. 1145–1153
- [25]. Paul, A., Subramanian, K., Sujitha, N.: 'PV-based off-board electric vehicle battery charger using BIDC', Turk. J. Electr. Eng. Comput. Sci., 2019, 27, (4), pp. 2850–2865
- [26]. Sree, L., Umamaheswari, M.G.: 'A Hankel matrix reduced order SEPIC model for simplified voltage control optimization and MPPT', Sol. Energy, 2018, 170, pp. 280–292
- [27]. Zhang, J.: 'Bidirectional DC-DC power converter design optimization, modeling and control'. Dissertation, the faculty of the Virginia Polytechnic Institute and State University, Virginia Polytechnic Institute and State University, 2008
- [28]. Gounden, N.G.A., Krithiga, S.: 'Power electronic configuration for the operation of PV system in combined grid-connected and stand-alone modes', IET Power Electron., 2014, 7, pp. 640–647
- [29]. Arul Daniel, S., Ammasai Gounden, N.: 'A novel hybrid isolated generating system based on PV fed inverter assisted wind driven induction generators', IEEE Trans. Energy Convers., 2004, 19, (2), pp. 416–422